ICES REPORT 12-39

August 2012

Discrete Spectrum Analyses for Various Mixed Discretizations of the Stokes Eigenproblem

by

John A. Evans and Thomas J.R. Hughes

The Institute for Computational Engineering and Sciences
The University of Texas at Austin
Austin, Texas 78712

Reference: John A. Evans and Thomas J.R. Hughes, Discrete Spectrum Analyses for Various Mixed Discretizations of the Stokes Eigenproblem, ICES REPORT 12-39, The Institute for Computational Engineering and Sciences, The University of Texas at Austin, August 2012.

Report Documentation Page

Form Approved
OMB No. 0704-0188

1. REPORT DATE	2. REPORT TYPE	3. DATES COVERED
AUG 2012		**00-00-2012 to 00-00-2012**

4. TITLE AND SUBTITLE	5a. CONTRACT NUMBER
Discrete Spectrum Analyses for Various Mixed Discretizations of the Stokes Eigenproblem	5b. GRANT NUMBER
	5c. PROGRAM ELEMENT NUMBER
6. AUTHOR(S)	5d. PROJECT NUMBER
	5e. TASK NUMBER
	5f. WORK UNIT NUMBER
7. PERFORMING ORGANIZATION NAME(S) AND ADDRESS(ES) **University of Texas at Austin,The Institute for Computational Engineering and Sciences,Austin,TX,78712**	8. PERFORMING ORGANIZATION REPORT NUMBER
9. SPONSORING/MONITORING AGENCY NAME(S) AND ADDRESS(ES)	10. SPONSOR/MONITOR'S ACRONYM(S)
	11. SPONSOR/MONITOR'S REPORT NUMBER(S)

12. DISTRIBUTION/AVAILABILITY STATEMENT
Approved for public release; distribution unlimited

13. SUPPLEMENTARY NOTES

14. ABSTRACT

We conduct discrete spectrum analyses for a selection of mixed discretization schemes for the Stokes eigenproblem. In particular, we consider the MINI el- ement, the Crouzeix-Raviart element, the Marker-and- Cell scheme, the Taylor-Hood element, the Qk=Pk&#56256;&#56320;1 el- ement, the divergence-conforming discontinuous Galerkin method, and divergence-conforming B-splines. For each of these schemes, we compare the spectrum for the con- tinuous Stokes problem with the spectrum for the dis- crete Stokes problem, and we discuss the relationship of eigenvalue errors with solution errors associated with unsteady viscous ow problems.

15. SUBJECT TERMS

16. SECURITY CLASSIFICATION OF:			17. LIMITATION OF ABSTRACT	18. NUMBER OF PAGES	19a. NAME OF RESPONSIBLE PERSON
a. REPORT **unclassified**	b. ABSTRACT **unclassified**	c. THIS PAGE **unclassified**	**Same as Report (SAR)**	**10**	

Computational Mechanics manuscript No.
(will be inserted by the editor)

Discrete Spectrum Analyses for Various Mixed Discretizations of the Stokes Eigenproblem

John A. Evans · Thomas J.R. Hughes

Received: date / Accepted: date

Abstract We conduct discrete spectrum analyses for a selection of mixed discretization schemes for the Stokes eigenproblem. In particular, we consider the MINI element, the Crouzeix-Raviart element, the Marker-and-Cell scheme, the Taylor-Hood element, the $\mathbf{Q}_k/P_{k-1}$ element, the divergence-conforming discontinuous Galerkin method, and divergence-conforming B-splines. For each of these schemes, we compare the spectrum for the continuous Stokes problem with the spectrum for the discrete Stokes problem, and we discuss the relationship of eigenvalue errors with solution errors associated with unsteady viscous flow problems.

Keywords Stokes eigenproblem · mixed methods · discrete spectrum analysis

1 Introduction

One of the most important roles of numerical analysis is to quantify the induced error of a particular discretization scheme. Classical *a priori* error estimation techniques allow one to identify the asymptotic convergence rate of a scheme, but they rarely give much insight into a method's pre-asymptotic characteristics. Alternatively, one may utilize discrete spectrum analysis to analyze the approximation properties of all the scales of a discretization scheme. In discrete spectrum analysis, one directly compares the spectrum of a chosen differential operator with the spectrum of the discretized version of the differential operator. Discrete spectrum analysis has a long history in structural dynamics where the eigenvalues of a linear structural system correspond to the squares of the natural frequencies [19]. For linear structural dynamics problems, it can be shown that errors in natural frequency lead to a linear accumulation of solution error in time which scales with frequency error. For nonlinear structural dynamics problems, induced coupling of low and high modes exacerbates this accumulation of error, ultimately resulting in non-robust numerical schemes. Hence, a discretization technique whose discrete spectrum closely matches the exact spectrum is highly desirable. Discrete spectrum analysis can also be utilized to analyze diffusive problems where the eigenvalues of the underly differential systems correspond to the dissipation rates of distinct eigenmodes [2]. While it can be easily shown that errors in dissipation rates do result in enlarged solution error, these errors typically decay exponentially in time. Nevertheless, quantification of such errors is important for diffusive problems exhibiting a wide array of spatial and temporal scales such as viscous turbulent fluid flow.

In this paper, we conduct a discrete spectrum analysis for a selection of mixed discretization schemes for the Stokes eigenproblem. For simplicity, we restrict our attention to the Stokes eigenproblem posed on the two-dimensional torus. The eigenvalues of the Stokes eigenproblem correspond to the dissipation rates of the natural modes of unsteady Stokes flow as well as the squares of the natural frequencies of linear incompressible elastodynamics. Furthermore, in the context of incompressible turbulent fluid flow, these eigenvalues approximately match the dissipation rates of modes with sufficiently high wave number, namely modes in the viscous range, and comprise a significant fraction of the dissipation rates of modes at the tail end of the inertial range. Consequently, a scheme with favorable resolution prop-

J.A. Evans · T.J.R. Hughes
Institute for Computational Engineering and Sciences
201 East 24th Street, Stop C0200
Austin, Texas 78712-1229
E-mail: evans@ices.utexas.edu

erties should be characterized by a discrete spectrum which closely mimics the exact spectrum.

An outline of this paper is as follows. In Section 2, we consider the unsteady Stokes flow problem and express its solution in terms of the eigenvalues and eigenmodes of the Stokes eigenproblem. We also discuss numerical approximation of the unsteady Stokes flow problem and its relationship to the Stokes eigenproblem, and we discuss estimation of solution errors. In Section 3, we conduct discrete spectrum analyses for a variety of mixed discretization schemes for the Stokes eigenproblem, starting with the MINI element in Subsection 3.1 and ending with divergence-conforming B-splines in Subsection 3.7. In Section 4, we draw conclusions.

2 Unsteady Stokes Flow and the Stokes Eigenproblem

To properly motivate discrete spectrum analysis and its role in characterizing errors associated with time-dependent problems, we consider the unsteady Stokes flow problem in this section and express its solution in terms of eigenvalues and eigenmodes. For simplicity, let us consider the unsteady Stokes problem on the two-dimensional torus subject to no applied forcing. To this effect, we set $\Omega = (0, 2\pi)^2$ and introduce the Sobolev spaces

$$\mathbf{H}^1_{per}(\Omega) := \{\, \mathbf{u} \in \mathbf{H}^1(\Omega) : \mathbf{u}(\cdot, 0) = \mathbf{u}(\cdot, 2\pi), \mathbf{u}(0, \cdot) = \mathbf{u}(2\pi, \cdot)\}$$

and

$$\mathbf{L}^2_{per}(\Omega) := L^2_0(\Omega).$$

Furthermore, for a given end-time $T > 0$, we define the spaces

$$\mathcal{V}_{T,per} := \{\, \mathbf{v} \in L^2(0, T; \mathbf{H}^1_{per}(\Omega)) : \partial_t \mathbf{v} \in L^2(0, T; \mathbf{H}^*_{per}(\Omega))\}$$

and

$$\mathcal{Q}_{T,per} := L^2(0, T; L^2_{per}(\Omega))$$

where $\mathbf{H}^*_{per}(\Omega)$ denotes the dual space of $\mathbf{H}^1_{per}(\Omega)$. Given $\mathbf{u}_0 \in \mathbf{H}^1_{per}(\Omega)$, the problem of interest then reads as follows.

$$(P) \left\{ \begin{array}{l} \text{Find } \mathbf{u} \in \mathcal{V}_{T,per} \text{ and } p \in \mathcal{Q}_{T,per} \text{ such that } \mathbf{u}(0) = \mathbf{u}_0 \text{ and, for almost every } t \in (0, T), \\ \\ \langle \partial_t \mathbf{u}(t), \mathbf{v} \rangle + k(\mathbf{u}(t), \mathbf{v}) - b(p(t), \mathbf{v}) \\ \qquad\qquad + b(q, \mathbf{u}(t)) = 0 \\ \\ \text{for all } \mathbf{v} \in \mathbf{H}^1_{per}(\Omega) \text{ and } q \in L^2_{per}(\Omega) \text{ where} \\ \\ k(\mathbf{u}, \mathbf{v}) = \nu \displaystyle\int_\Omega \nabla \mathbf{u} : \nabla \mathbf{v} d\mathbf{x}, \\ \\ b(p, \mathbf{v}) = \displaystyle\int_\Omega p \nabla \cdot \mathbf{v} d\mathbf{x}. \end{array} \right.$$

Above, $\mathbf{u}$ denotes the flow velocity of a fluid moving through the domain Ω, p denotes the pressure acting on the fluid divided by the fluid density, and ν denotes the kinematic viscosity of the fluid. Problem (P) consists of an evolutionary equation subject only to dissipation in time. Now, defining the space of divergence-free functions as

$$\mathring{\mathbf{H}}^1_{per}(\Omega) := \left\{ \mathbf{v} \in \mathbf{H}^1_{per}(\Omega) : \nabla \cdot \mathbf{v} = 0 \right\},$$

let us consider the following eigenproblem.

$$(E) \left\{ \begin{array}{l} \text{Find } \widehat{\mathbf{u}} \in \mathring{\mathbf{H}}^1_{per}(\Omega) \text{ and } \lambda \in \mathbb{R}^+ \text{ such that } \|\widehat{\mathbf{u}}\|_{\mathbf{L}^2(\Omega)} = 1 \text{ and} \\ \\ k(\widehat{\mathbf{u}}, \mathbf{v}) = \lambda \left(\widehat{\mathbf{u}}, \mathbf{v}\right)_{\mathbf{L}^2(\Omega)} \\ \\ \text{for all } \mathbf{v} \in \mathring{\mathbf{H}}^1_{per}(\Omega). \end{array} \right.$$

The orthonormal eigenmodes corresponding to the above problem are explicitly known and comprise the set

$$\{\, \widehat{\mathbf{u}} = \frac{\text{curl}\phi}{\|\text{curl}\phi\|_{\mathbf{L}^2(\Omega)}} : \phi = \exp\left(ik_1 x + ik_2 y\right), \\ k_1, k_2 \in \mathbb{Z}, k_1^2 + k_2^2 \neq 0 \}.$$

We enumerate these eigenmodes and their corresponding eigenvalues as $\{\widehat{\mathbf{u}}_n, \lambda_n\}_{n=1}^\infty$ where

$$\lambda_1 \leq \lambda_2 \leq \cdots.$$

Finally, a direct calculation shows that the exact velocity solution of (P) can be written as

$$\mathbf{u}(\mathbf{x}, t) = \mathbf{A}_0 + \sum_{n=1}^{\infty} A_n \widehat{\mathbf{u}}_n(\mathbf{x}) \exp(-\lambda_n t)$$

where

$$\mathbf{A}_0 = \int_\Omega \mathbf{u}_0(\mathbf{x}) d\mathbf{x}$$

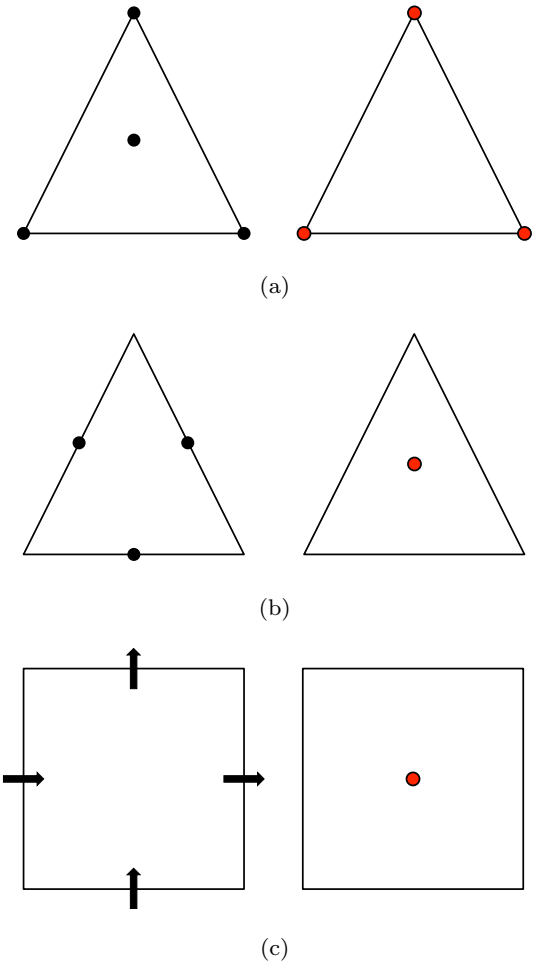

Fig. 1 Degrees of freedom: (a) the MINI element, (b) the non-conforming Crouzeix-Raviart element, (c) the Marker-and-Cell finite difference scheme. Velocity DOF are on the left and pressure DOF are on the right.

and

$$A_n = \int_\Omega \mathbf{u}_0(\mathbf{x}) \cdot \widehat{\mathbf{u}}_n(\mathbf{x}) d\mathbf{x}.$$

Hence, the velocity solution of (P) depends only on the initial condition $\mathbf{u}_0$, the eigenmodes $\{\widehat{\mathbf{u}}_n\}_{n=1}^{\infty}$, and the eigenvalues $\{\lambda_n\}_{n=1}^{\infty}$. Furthermore, the eigenvalues $\{\lambda_n\}_{n=1}^{\infty}$ gives the dissipation rates of the individual eigenmodes. We may repeat all of the above calculations at the discrete level to express our discrete velocity solution entirely in terms of the discrete initial condition $\mathbf{u}_{0,h}$, discrete eigenmodes $\left\{\widehat{\mathbf{u}}_n^h\right\}_{n=1}^{N}$, and discrete eigenvalues $\left\{\lambda_n^h\right\}_{n=1}^{N}$ where N denotes the total number of discretely divergence-free modes corresponding to nonzero eigenvalues. A natural question to then ask is how well do the discrete eigenvalues approximate the first N exact eigenvalues. This question can be answered to some degree using tools arising from functional analysis. For example, it is well-known that the discrete eigenvalues arising from a conforming, stable, and balanced mixed finite element approximation of the Stokes eigenproblem satisfy the relationship

$$|\lambda_n - \lambda_n^h| \leq Ch^{2k}$$

provided the product nh is sufficiently small where h is the mesh size, k is the polynomial degree of the discrete velocity space, and C is a positive constant independent of h [4]. Unfortunately, this relationship only gives an error bound for discrete eigenvalues corresponding to the lowest discrete eigenmodes. For simple eigenproblems such as those arising from one-dimensional structural dynamics, one can employ discrete Fourier analysis to exactly characterize discrete eigenvalue errors across the entire spectrum [21], though this analysis is intractable in the context of multi-dimensional Stokes flow. Hence, in this paper, we resort to direct computation to compute discrete eigenvalue errors and compare discrete spectra with the spectrum corresponding to the continuous Stokes eigenproblem.

3 Discrete Spectrum Analyses

3.1 The MINI Element

We begin our discrete spectrum analyses with the so-called MINI element. Originally introduced by Arnold, Brezzi, and Fortin in [1], the MINI element is arguably the most efficient mixed discretization scheme for the approximation of Stokes flow. The velocity space of the MINI element is defined to be that of piecewise continuous linears enriched by the space of element-wise cubic bubbles over a given triangulation, and the pressure space is defined to be only that of piecewise continuous linears. The degrees of freedom (DOF) for this element are illustrated in Fig. 1(a). It should be noted that if one statically condenses the cubic bubbles over each element, one arrives at a formulation that is nearly algebraically equivalent to the pressure-stabilized $\mathbf{P}_1/P_1$ velocity/pressure pair [20].

We have computed the discrete Stokes spectrum corresponding to the MINI element on a structured triangular mesh with 1,568 elements and plotted a comparison of the discrete spectrum with the exact spectrum in Fig. 2. In the figure, n denotes the given mode number while N denotes the total number of discrete modes. For this calculation, $N = 3,919$. Note that while the initial part of the spectrum is fairly well-resolved, the discrete eigenvalues corresponding to $n/N > 0.15$ exhibit more than fifty percent error. As the discrete

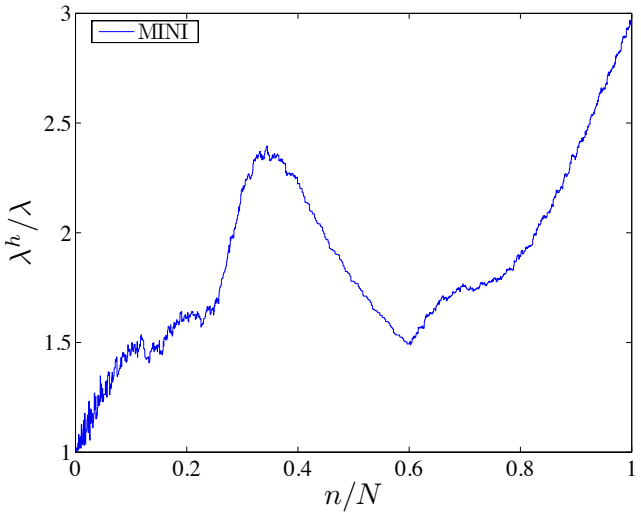

Fig. 2 Stokes spectrum for the MINI element.

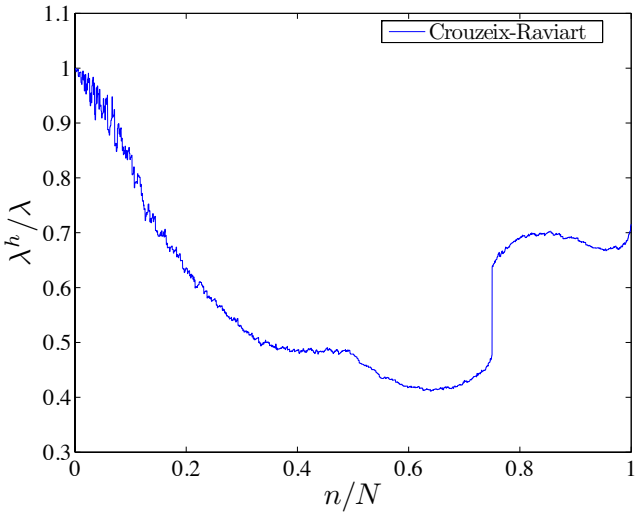

Fig. 3 Stokes spectrum for the Crouzeix-Raviart element.

eigenvalues are larger in magnitude than the continuous eigenvalues, this indicates that in an unsteady flow simulation, eighty five percent of the discrete modes will dissipate much faster than their continuous counterparts. It should be indicated that the upper part of the discrete spectrum exhibits nearly two hundred percent error. Finally, we have also computed the discrete Stokes spectrum for a wide variety of mesh resolutions and found similar results to those reported here. This is also the case for the other discretization schemes considered in this paper.

3.2 The Non-conforming Crouzeix-Raviart Element

We proceed by conducting a discrete spectrum analysis for the non-conforming Crouzeix-Raviart element [11]. For this element, midside nodes are used as DOF for the discrete velocity field. This generates a non-conforming piecewise linear approximation. The discrete pressure field is taken to be constant on each element. The DOF for this element are illustrated in Fig. 1(b). As the divergence of the discrete velocity field is piecewise constant, this velocity/pressure pair results in a discrete velocity field which is exactly divergence-free over each element. Furthermore, the non-conforming Crouzeix-Raviart element admits an element-wise mass conservation law in the sense that the total amount of mass which flows out of the element is equal to the total amount of mass which flows in. However, the element is not strongly mass-conservative as the discrete velocity field associated with the element does not exhibit normal continuity across element boundaries. Like the MINI element, the non-conforming Crouzeix-Raviart element is computationally inexpensive and popular in practice, though it is generally less robust than the MINI element. For example, the discretized momentum equation associated with the non-conforming Crouzeix-Raviart element is not coercive in the presence of traction boundary conditions.

We have computed the discrete Stokes spectrum corresponding to the non-conforming Crouzeix-Raviart element on a structured triangular mesh with 2,048 elements and plotted a comparison of the discrete spectrum with the exact spectrum in Fig. 3. For this calculation, $N = 4,095$. Note that all of the discrete eigenvalues are smaller in magnitude than their continuous counterpart. This indicates that, in an unsteady flow simulation, all of the discrete modes will dissipate slower than their continuous counterparts. In a turbulent flow simulation free of turbulence models, this will have the effect of lengthening the discrete inertial range and pushing back the discrete viscous range to higher wavenumbers. Furthermore, while most of the discrete eigenvalues exhibit less than fifty percent error, less than ten percent of the discrete eigenvalues exhibit less than ten percent error.

3.3 The Marker-and-Cell Scheme

We next consider the Marker-and-Cell (MAC) finite difference scheme. The MAC scheme is one of the oldest schemes for incompressible fluid flow and was originally introduced by Harlow and Welch to simulate free-surface problems [17]. In the MAC scheme, the velocity field is defined on cell faces, the pressure field is defined on cell interiors, and finite differences are utilized to discretize the momentum equation on cell faces and the continuity equation on cell interiors. The DOF

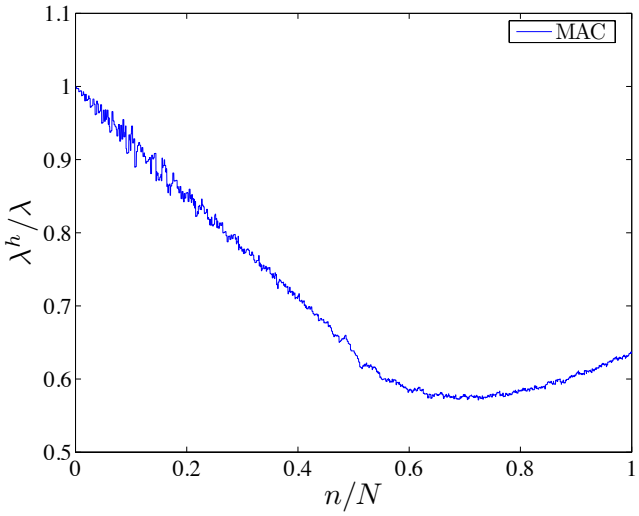

Fig. 4 Stokes spectrum for the Marker-and-Cell scheme.

for this scheme are illustrated in Fig. 1(c). The MAC scheme has been shown to be equivalent to a finite element scheme [24], a mixed finite element method in vorticity-velocity-pressure formulation with special numerical quadrature [16], and a particular divergence-conforming discontinuous Galerkin method [22]. The MAC scheme satisfies a mass conservation statement on each cell by construction, and this conservation property has resulted in enhanced robustness for problems where mass conservation is of critical importance such as coupled fluid-transport [23].

We have computed the discrete Stokes spectrum corresponding to the MAC scheme on a structured rectangular mesh with 4,096 elements and plotted a comparison of the discrete spectrum with the exact spectrum in Fig. 4. For this calculation, $N = 4,095$. Note that all of the discrete eigenvalues are smaller than their continuous counterpart as was the case for the non-conforming Crouzeix-Raviart element. Hence, they will suffer from the same issues as the Crouzeix-Raviart element. Namely, in a turbulent flow simulation without the introduction of turbulence models, the discrete inertial range will be artificially lengthened. However, for the most part, the discrete spectrum corresponding to the MAC scheme is better resolved than that of the Crouzeix-Raviart element. Approximately ten percent of the discrete eigenvalues exhibit less than ten percent error.

3.4 The Taylor-Hood Family

We continue by conducting discrete spectrum analyses for the Taylor-Hood family of Stokes elements [18]. For a given polynomial degree $k \geq 2$, the velocity field is approximated by continuous piecewise tensor-product polynomials of degree k and the pressure field is approximated by continuous piecewise tensor-product polynomials of degree $k-1$. We denote this velocity/pressure pair as $\mathbf{Q}_k/Q_{k-1}$. The DOF for the second-order Taylor-Hood pair $\mathbf{Q}_2/Q_1$ are illustrated in Fig. 5(a). The second-order Taylor-Hood pair is one of the most popular finite elements for incompressible flow simulation. It is balanced in the sense that the discrete velocity field is second-order accurate in the $\mathbf{H}^1$-norm and the discrete pressure field is second-order accurate in the L^2-norm. Mixed finite elements which are unbalanced typically suffer from suboptimal convergence.

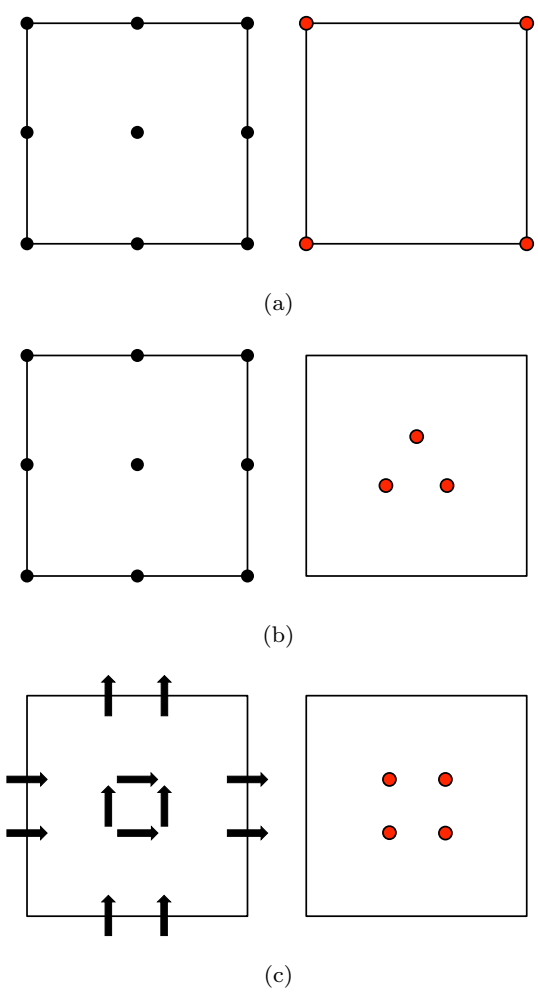

Fig. 5 Degrees of freedom: (a) the second-order Taylor-Hood pair, (b) the $\mathbf{Q}_2/P_1$ pair, (c) the second-order Raviart-Thomas pair. Velocity DOF are on the left and pressure DOF are on the right.

For $k = 2, 3, 4, 5$, we have computed the discrete Stokes spectrum corresponding to the $\mathbf{Q}_k/Q_{k-1}$ element on a structured rectangular mesh and plotted a comparison of the discrete spectrum with the ex-

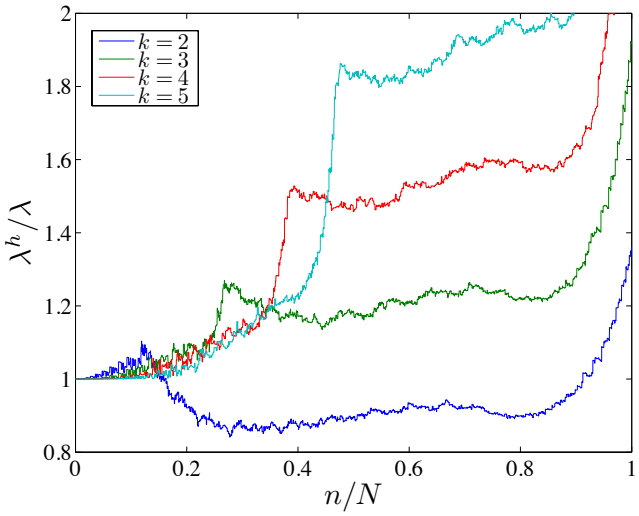

Fig. 6 Stokes spectrum for the Taylor-Hood family.

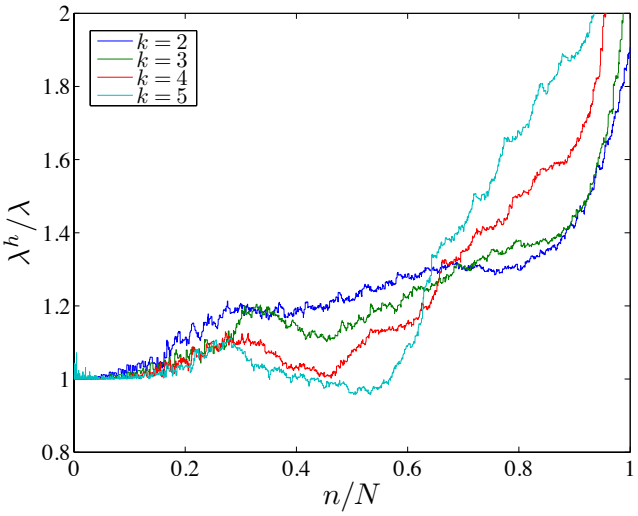

Fig. 7 Stokes spectrum for the $\mathbf{Q}_k/P_{k-1}$ family.

act spectrum in Fig. 6. For each polynomial degree, we chose a sufficiently fine mesh such that $N \approx 4000$. Note that the initial portion of the discrete spectrum improves dramatically with increased polynomial degree. This is expected from classical *a priori* error estimates. Asymptotically, discrete eigenvalues converge like h^{2k} for the Taylor-Hood family. However, the entire discrete spectrum does not improve with increased polynomial degree. In fact, the upper part of the discrete spectrum worsens. This indicates that the high modes of the discrete Stokes system have no approximability and these modes get worse with increased polynomial degree. This is analogous to what has been observed for *hp*-finite elements in the context of structural dynamics [21]. Furthermore, it should be noted that many of the discrete eigenvalues corresponding to the $\mathbf{Q}_2/Q_1$ pair are smaller than their continuous counterpart.

3.5 The $\mathbf{Q}_k/P_{k-1}$ Family

We next consider the $\mathbf{Q}_k/P_{k-1}$ family of Stokes elements [3]. In this discretization scheme, the velocity field is approximated using continuous piecewise tensor-product polynomials of degree k and the pressure field is approximated using discontinuous piecewise polynomials of degree $k-1$. The DOF for the second-order member of the family are illustrated in Fig. 5(b). Like the Taylor-Hood pairs, the $\mathbf{Q}_k/P_{k-1}$ pair is balanced. Furthermore, as the discrete pressure field contains piecewise constants, the discrete velocity field arising from a $\mathbf{Q}_k/P_{k-1}$ discretization is mass-conservative element-by-element. Like the MAC scheme, this conservation property has resulted in enhanced robustness for problems where mass conservation is of importance.

For $k = 2, 3, 4, 5$, we have computed the discrete Stokes spectrum corresponding to the $\mathbf{Q}_k/P_{k-1}$ on a structured rectangular mesh and plotted a comparison of the discrete spectrum with the exact spectrum in Fig. 7. For each polynomial degree, we chose a sufficiently fine mesh such that $N \approx 4000$. Note immediately that the discrete spectra associated with these discretizations are somewhat erratic and unpredictable. Like the Taylor-Hood family of discretizations, the initial portion of the discrete spectrum improves with increasing polynomial degree and the upper part worsens. Moreover, as the polynomial degree is increased, the middle portion of the discrete spectrum is driven to be smaller and smaller. This being said, for a given polynomial degree k, the discrete spectrum associated with the $\mathbf{Q}_k/P_{k-1}$ finite element pair is generally more accurate than the discrete spectrum associated with the $\mathbf{Q}_k/Q_{k-1}$ pair.

3.6 Divergence-conforming DG Elements

We proceed by conducting discrete spectrum analyses for divergence-conforming discontinuous Galerkin (DG) schemes which arise when one employs a Raviart-Thomas velocity/pressure pair in conjunction with the symmetric interior penalty Galerkin method to enforce tangential continuity across element faces [8,9,22]. Such schemes have become increasingly popular in recent years as they result in discrete velocity fields which are pointwise divergence-free. In the context of Navier-Stokes flow, exact satisfaction of the incompressibility constraint guarantees that divergence-conforming DG schemes automatically conserve momentum and are energy stable. The DOF associated with the second-order

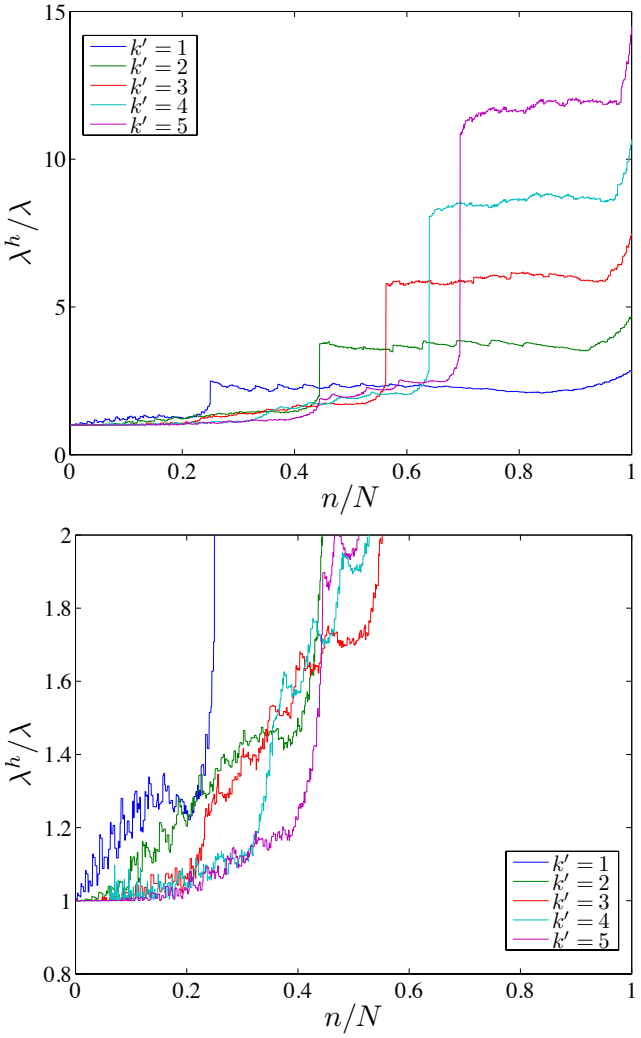

Fig. 8 Stokes spectrum for divergence-conforming DG elements. Top: global view, bottom: zoomed in view.

Raviart-Thomas pair are depicted in Fig. 5(c). It should be noted that in the context of Stokes flow, the classical second-order Raviart-Thomas pair is only first-order accurate as the discrete space of velocity fields associated with the second-order Raviart-Thomas pair is complete only up to linear polynomials. For this reason, we will designate the divergence-conforming DG scheme employing a k^{th}-order Raviart-Thomas velocity/pressure pair as $(k')^{th} = (k-1)^{th}$-order.

For $k' = 1, 2, 3, 4, 5$, we have computed the discrete Stokes spectrum corresponding to the $(k')^{th}$-order divergence-conforming DG scheme on a structured rectangular mesh and plotted a comparison of the discrete spectrum with the exact spectrum in Fig. 8. For each polynomial degree, we chose a sufficiently fine mesh such that $N \approx 4000$, and we selected the interior penalty parameter as $4(k'+1)^2$. Note from the figure that while the initial portion of the discrete spectrum improves

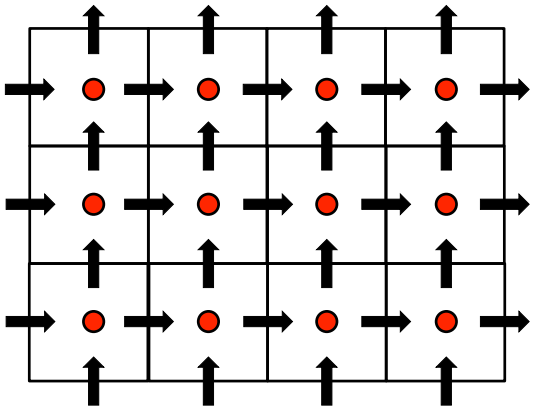

Fig. 9 Degrees of freedom: divergence-conforming B-splines. Velocity DOF are designated by arrows and pressure DOF are designated by points.

with increased polynomial degree, the upper part of the spectrum catastrophically worsens. Furthermore, we found the quality of the discrete spectrum degraded with increasing interior penalty parameter. This indicates that one should choose the interior penalty parameter intelligently not only for the purposes of numerical stability but also for numerical accuracy. Unfortunately, this fact is not often elaborated in the literature.

3.7 Divergence-conforming B-splines

We finish by conducting discrete spectrum analyses for divergence-conforming B-spline approximations of the Stokes eigenproblem [5,12]. These approximations are motivated by the recent theory of isogeometric discrete differential forms [6,7] and may be interpreted as smooth generalizations of Raviart-Thomas elements. As these approximations are smooth, they can be directly utilized in the Galerkin solution of viscous flows without resorting to a DG technology in contrast with classical Raviart-Thomas elements. Recent work has shown these approximations are much more accurate and stable than classical methods for Stokes and Navier-Stokes flows [13–15]. Furthermore, in the context of Navier-Stokes flow, these approximations admit balance laws for momentum, energy, vorticity, enstrophy, and helicity as they satisfy the incompressibility constraint exactly [15]. Since divergence-conforming B-spline approximations exhibit additional smoothness in comparison with classical finite elements, it is not possible to attribute DOF to element quantities. Instead, DOF can be identified to cells and edges on a global data structure called a control mesh. For reference, see Chapter 4

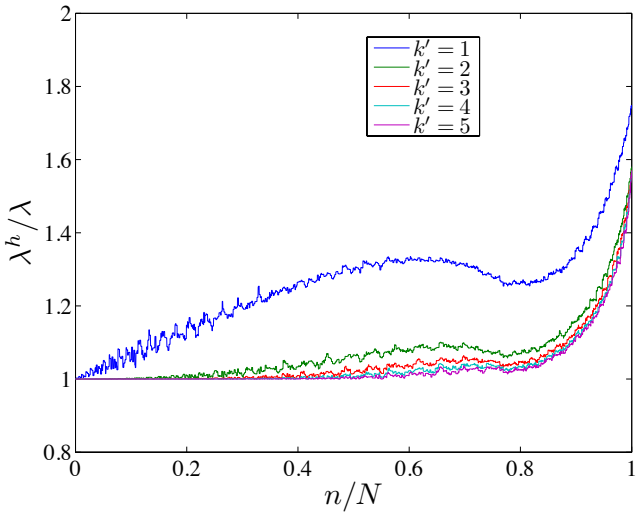

Fig. 10 Stokes spectrum for divergence-conforming B-splines.

of [12] or Chapter 2 of [10]. We have depicted a standard DOF pattern on a patch in Fig. 9. Note the similarity of the DOF structure with that of the MAC scheme.

For $k' = 1, 2, 3, 4, 5$, we have computed the discrete Stokes spectrum corresponding to the $(k')^{th}$-order divergence-conforming B-spline scheme on a structured rectangular mesh with $4,096$ elements and plotted a comparison of the discrete spectrum with the exact spectrum in Fig. 10. For these calculations, $N = 4,095$. Note that the discrete spectrum is quite well-resolved for all polynomial degrees and that the entire discrete spectrum improves markedly with increasing polynomial degree. The discrete spectrum corresponding to the first-order B-spline discretization is remarkably more accurate than the discrete spectra corresponding to the other first-order methods in this paper (the MINI element, the Crouzeix-Raviart element, the MAC scheme, and the first-order divergence-conforming DG scheme), and the discrete spectrum corresponding to the second-order B-spline discretization is dramatically more accurate than the discrete spectrum associated with any other method considered in this paper. In fact, approximately eighty five percent of the spectrum exhibits less than ten percent error for the second-order B-spline discretization, and approximately eighty five percent of the spectrum exhibits less than four percent error for the fifth-order B-spline discretization. We should finally mention that all of the discrete eigenvalues associated with a divergence-conforming B-spline approximation necessarily satisfy $\lambda_n^h \geq \lambda_n$ since the approximation scheme is a conforming interior approximation technique (i.e., divergence-conforming B-spline schemes deliver discrete velocity fields which are pointwise divergence-free).

4 Conclusions

In this paper, discrete spectrum analyses were conducted for a selection of mixed discretization schemes for the Stokes eigenproblem. These analyses revealed that classical schemes such as the MINI element, the non-conforming Crouzieux-Raviart element, and the Marker-in-Cell scheme exhibit poorly resolved discrete spectra, and they further revealed that the upper part of the discrete spectrum degraded under degree elevation for Taylor-Hood elements, $\mathbf{Q}_k/P_{k-1}$ elements, and divergence-conforming DG elements. This is concerning as the eigenvalues of the Stokes eigenproblem correspond to the dissipation rates of the natural modes of unsteady Stokes flow as well as the squares of the natural frequencies of linear incompressible elastodynamics. Consequently, a scheme with favorable resolution properties should be characterized by a discrete spectrum which closely mimics the exact spectrum. In contrast with the other methods studied in this paper, it was discovered that the discrete spectrum associated with divergence-conforming B-spline approximations is quite well-resolved for all polynomial degrees and that the entire discrete spectrum improves markedly with increasing polynomial degree. This motivates further study of divergence-conforming B-spline approximations in the context of fluid flow simulation and incompressible elastodynamics.

Acknowledgements John A. Evans and Thomas J.R. Hughes were partially supported by the Office of Naval Research under contract number N00014-08-0992. John A. Evans was additionally partially supported by the Department of Energy Computational Science Graduate Fellowship, provided under grant number DE-FG02-97ER25308. This support is gratefully acknowledged.

References

1. Arnold, D.N., Brezzi, F., Fortin, M.: A stable finite element for the Stokes equations. Calcolo **21**, 337–344 (1984)
2. Bazilevs, Y., Calo, V.M., Cottrell, J.A., Hughes, T.J.R., Reali, A., Scovazzi, G.: Variational multiscale residual-based turbulence modeling for large eddy simulation of incompressible flows. Computer Methods in Applied Mechanics and Engineering **197**, 173–201 (2007)
3. Bernardi, C., Maday, Y.: Uniform inf-sup conditions for the spectral discretization of the Stokes problem. Mathematical Models and Methods in Applied Sciences **9**, 395–414 (1999)
4. Boffi, D.: Finite element approximation of eigenvalue problems. Acta Numerica **19**, 1–120 (2010)
5. Buffa, A., de Falco, C., Vázquez, R.: Isogeometric analysis: Stable elements for the 2D Stokes equation. International Journal for Numerical Methods in Fluids **65**, 1407–1422,20–30 (2011)

6. Buffa, A., Rivas, J., Sangalli, G., Vázquez, R.: Isogeometric discrete differential forms in three dimensions. SIAM Journal on Numerical Analysis **49**, 818–844 (2011)
7. Buffa, A., Sangalli, G., Vázquez, R.: Isogeometric analysis in electromagnetics: B-splines approximation. Computer Methods in Applied Mechanics and Engineering **199**, 1143–1152 (2010)
8. Cockburn, B., Kanschat, G., Schötzau, D.: A locally conservative LDG method for the incompressible Navier-Stokes equations. Mathematics of Computation **74**, 1067–1095 (2004)
9. Cockburn, B., Kanschat, G., Schötzau, D.: A note on discontinuous Galerkin divergence-free solutions of the Navier-Stokes equations. SIAM Journal on Scientific Computing **31**, 61–73 (2007)
10. Cottrell, J.A., Hughes, T.J.R., Bazilevs, Y.: Isogeometric Analysis: Toward Integration of CAD and FEA. Wiley (2009)
11. Crouzeix, M., Raviart, P.A.: Conforming and nonconforming finite element methods for solving the stationary Stokes equations. R.A.I.R.O. Analyse Numérique **7**, 33–76 (1973)
12. Evans, J.A.: Divergence-free B-spline Discretizations for Viscous Incompressible Flows. Ph.D. thesis, The University of Texas at Austin (2011)
13. Evans, J.A., Hughes, T.J.R.: Isogeometric divergence-conforming B-splines for the Darcy-Stokes-Brinkman Equations. Mathematical Models and Methods in Applied Sciences (2012). In press.
14. Evans, J.A., Hughes, T.J.R.: Isogeometric divergence-conforming B-splines for the steady Navier-Stokes Equations. Tech. rep., ICES Report 12-15 (2012)
15. Evans, J.A., Hughes, T.J.R.: Isogeometric divergence-conforming B-splines for the steady Navier-Stokes Equations. Tech. rep., ICES Report 12-16 (2012)
16. Girault, V., Lopez, H.: Finite-element error estimates for the MAC scheme. IMA Journal of Numerical Analysis **16**, 347–379 (1996)
17. Harlow, F.H., Welch, J.E.: Numerical calculation of time-dependent viscous incompressible flow of fluid with free surface. Physics of Fluids **8**, 2182 (1965)
18. Hood, P., Taylor, C.: Navier-Stokes equations using mixed interpolation. In: J.T. Oden, R.H. Gallagher, O.C. Zienkiewicz, C. Taylor (eds.) Finite Element Methods in Flow Problems, pp. 121–132. University of Alabama in Huntsville Press (1974)
19. Hughes, T.J.R.: The Finite Element Method: Linear Static and Dynamic Finite Element Analysis. Dover Publications (2000)
20. Hughes, T.J.R., Franca, L.P., Balestra, M.: A new finite element formulation for computational fluid dynamics: V. Circumventing the Babuška-Brezzi condition: A stable Petrov-Galerkin formulation of the Stokes problem accomodating equal-order interpolations. Computer Methods in Applied Mechanics and Engineering **59**, 85–99 (1986)
21. Hughes, T.J.R., Reali, A., Sangalli, G.: Duality and unified analysis of discrete approximations in structural dynamics and wave propagation: Comparison of p-method finite elements with k-method NURBS. Computer Methods in Applied Mechanics and Engineering **197**, 4104–4124 (2008)
22. Kanschat, G.: Divergence-free discontinuous Galerkin schemes for the Stokes equations and the MAC scheme. International Journal for Numerical Methods in Fluids **56**, 941–950 (2008)
23. Matthies, G., Tobiska, L.: Mass conservation of finite element methods for coupled flow-transport problems. International Journal for Computing Science and Mathematics **1**, 293–307 (2007)
24. Nicolaides, R.A.: Analysis and convergence of the MAC scheme I. The linear problem. SIAM Journal on Numerical Analysis **29**, 1579–1591 (1992)